

AD-A124 687

EFFECTS OF CONDUCTION BAND ANISOTROPY ON THE  
EXCITON-PLASMA MOTT TRANSITION. (U) AIR FORCE INST OF  
TECH WRIGHT-PATTERSON AFB OH SCHOOL OF ENGI.  
B S DAVIES DEC 82 AFIT/GEP/PH/82D-7

1/1

UNCLASSIFIED

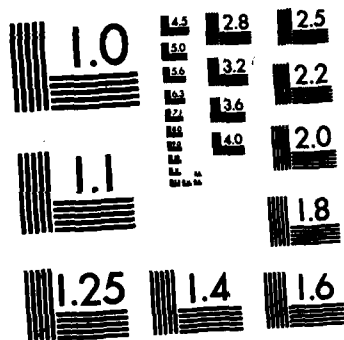
F/G 28/12 NL

END

FORMED

+

DTIC



MICROCOPY RESOLUTION TEST CHART  
NATIONAL BUREAU OF STANDARDS-1963-A

ADA 124687

# AIR FORCE INSTITUTE OF TECHNOLOGY



AIR UNIVERSITY  
UNITED STATES AIR FORCE

EFFECTS OF CONDUCTION BAND ANISOTROPY  
ON THE EXCITON-PLASMA MOTT TRANSITION  
IN INDIRECT GAP SEMICONDUCTORS

THESIS

AFIT/GEP/PH/82D-7

Barry S. Davies  
2nd Lt USAF

DTIC  
ELECTE  
FEB 22 1983

SCHOOL OF ENGINEERING

A

PATTERSON AIR FORCE BASE, OHIO

This document has been approved  
for public release and sale in  
distribution is unlimited

88-02-1021

AFIT/GEP/PH/82D-7

EFFECTS OF CONDUCTION BAND ANISOTROPY  
ON THE EXCITON-PLASMA MOTT TRANSITION  
IN INDIRECT GAP SEMICONDUCTORS

THESIS

AFIT/GEP/PH/82D-7

Barry S. Davies  
2nd Lt USAF

DTIC  
ELECTE  
FEB 22 1983  
S A D

Approved for public release; distribution unlimited

**AFIT/GEP/PH/82D-7**

# EFFECTS OF CONDUCTION BAND ANISOTROPY ON THE EXCITON-PLASMA MOTT TRANSITION IN INDIRECT GAP SEMICONDUCTORS

# THESIS

**Presented to the Faculty of the School of Engineering  
of the Air Force Institute of Technology  
Air University  
in Partial Fulfillment of the  
Requirements for the Degree of  
Master of Science**

by

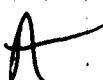
**Barry S. Davies**

**2nd Lt            USAF**

## Graduate Engineering Physics

**December 1982**

Approved for public release; distribution unlimited

Distribution For \_\_\_\_\_  
 INFO GRA&I ☒  
 INFO TAP ☐  
 Unannounced ☐  
 Justification \_\_\_\_\_  
 \_\_\_\_\_  
 \_\_\_\_\_  
 Distribution/  
 Avail. City Codes  
 \_\_\_\_\_  
 \_\_\_\_\_  
 Dist Special  




### Acknowledgments

Special thanks and credit should go to several people without whose participation this project would never have been completed.

Captain George Norris provided the day-to-day supervision. His knowledge of both the big-picture and the fine details of the project, and his willingness and ability to impart that knowledge, enabled me to accomplish far more than would have been possible otherwise.

Dr. K. K. Bajaj approved the project initially, provided several helpful discussions along the way, and made essential suggestions for the oral presentation.

Dr. Shankland contributed computer routines for numerical integration and function minimization. Also, my discussions with Dr. Shankland made the numerical analysis and programming problems easy where they would have been quite difficult otherwise.

Captain Dwight Phelps provided the key suggestion for finding the value of a non-tabulated integral.

Finally, special thanks should go to Jill Rueger for the typing of the final draft. Certainly there are few people who could do so much, so fast, so late.

## Contents

Acknowledgments . . . . .	ii
List of Figures . . . . .	iv
List of Tables . . . . .	v
Abstract . . . . .	vi
I. Introduction . . . . .	1
Exciton Formation . . . . .	2
The Exciton-Plasma Mott Transition . . . . .	3
II. Experiment . . . . .	5
Luminescence Spectra . . . . .	7
The Threshold Pumping Powers . . . . .	10
The Phase Diagram . . . . .	13
The Theoretical Problem . . . . .	14
III. Theory . . . . .	15
Background . . . . .	15
The Exciton Hamiltonian . . . . .	18
The Variational Calculation . . . . .	24
The Kinetic Energy: $\langle T \rangle$ . . . . .	25
The Potential Energy: $\langle V \rangle$ . . . . .	26
Minimization of the Total Energy . . . . .	32
IV. Results . . . . .	34
V. Summary and Conclusions . . . . .	39
Bibliography . . . . .	40
Appendix: The Anisotropic Dielectric Function . . . . .	42

## List of Figures


Figure		Page
1	Exciton Formation . . . . .	3
2	Phase Diagram . . . . .	6
3	Luminescence Spectra (18°K) . . . . .	8
4	Luminescence Spectra (23°K) . . . . .	9
5	Luminescence Spectra (30°K) . . . . .	11
6	Determination of Threshold Powers . . . . .	12



## List of Tables


Table		Page
I	Material Parameters . . . . .	35
II	Mott Transition in Si . . . . .	36
III	Mott Transition in Ge . . . . .	37
IV	Binding Energies for Zero Screening . . . . .	38

## Abstract



A theory is developed for the incorporation of conduction band anisotropy into the analysis of the exciton-plasma Mott transition in indirect gap semiconductors. Ellipsoidal energy surfaces are assumed for the electrons while spherical energy surfaces are retained for holes. Static electron-hole screening in the random phase approximation is assumed. The Mott transition is associated with the electron-hole pair density at which the exciton binding energy in the assumed potential is zero. The binding energy is computed variationally.

It is found that the electron anisotropy causes the Mott transition to shift to higher densities. It is also found that, in the absence of screening, the exciton binding energy is not significantly affected by the electron anisotropy. It is thus concluded that the shift to higher densities is due largely to the reduced ability of anisotropic electrons to screen.



# EFFECTS OF CONDUCTION BAND ANISOTROPY ON THE EXCITON-PLASMA MOTT TRANSITION IN INDIRECT GAP SEMICONDUCTORS

## I. Introduction

The exciton-plasma Mott transition in silicon has been studied in detail in recent years. The experimental data (Forchel, 1982; Forchel, to be published) has been successfully explained (Norris and Bajaj, 1982) by assuming that the electron-hole interaction is statically screened, and by taking the conduction and valence bands to be isotropic. While the assumption of conduction band isotropy works well in Si, where the ratio of longitudinal to transverse electron masses is less than five, one would expect the effects of conduction band anisotropy to be larger in Ge, where the ratio of longitudinal to transverse electron masses is greater than nineteen. It is thus the purpose of this work to extend the previously mentioned theory by taking conduction band anisotropy into account.

The system under study here consists of optically generated electron-hole (E-H) pairs in pure indirect gap semiconductors. The presentation will therefore begin with a discussion of how excitons are formed through optical pumping, followed by the definition of the exciton-plasma Mott transition.

In the next chapter, the experimental work will be discussed. This will be done to show the experimental

evidence for the occurrence of the exciton-plasma Mott transition, and to show clearly how the connection between theory and experiment is made.

The theory will be developed in chapter three and results for both Si and Ge will be presented in chapter four. Finally, the conclusions will be summarized in chapter five.

### Exciton Formation

The formation of excitons in an indirect gap semiconductor is shown schematically in Figure 1 (Wolfe, 1982). A photon, which has an energy greater than the energy gap ( $E_g$ ) of the semiconductor, is absorbed and excites an electron from the valence band to a conduction band state which lies above the conduction band minimum. The electron then undergoes a rapid thermalization process in which it loses energy to the lattice through the emission of phonons and thus relaxes to the conduction band minimum. Hydrogen-like bound states exist within the energy gap. They are due to bound E-H pairs, which are called excitons, and which may form if the sample is sufficiently cool (e.g.  $T < 80^\circ\text{K}$  for Si). The electron and hole eventually recombine giving off a characteristic luminescence. Since the material is indirect gap, the E-H recombination is also accompanied by the emission or absorption of phonons.

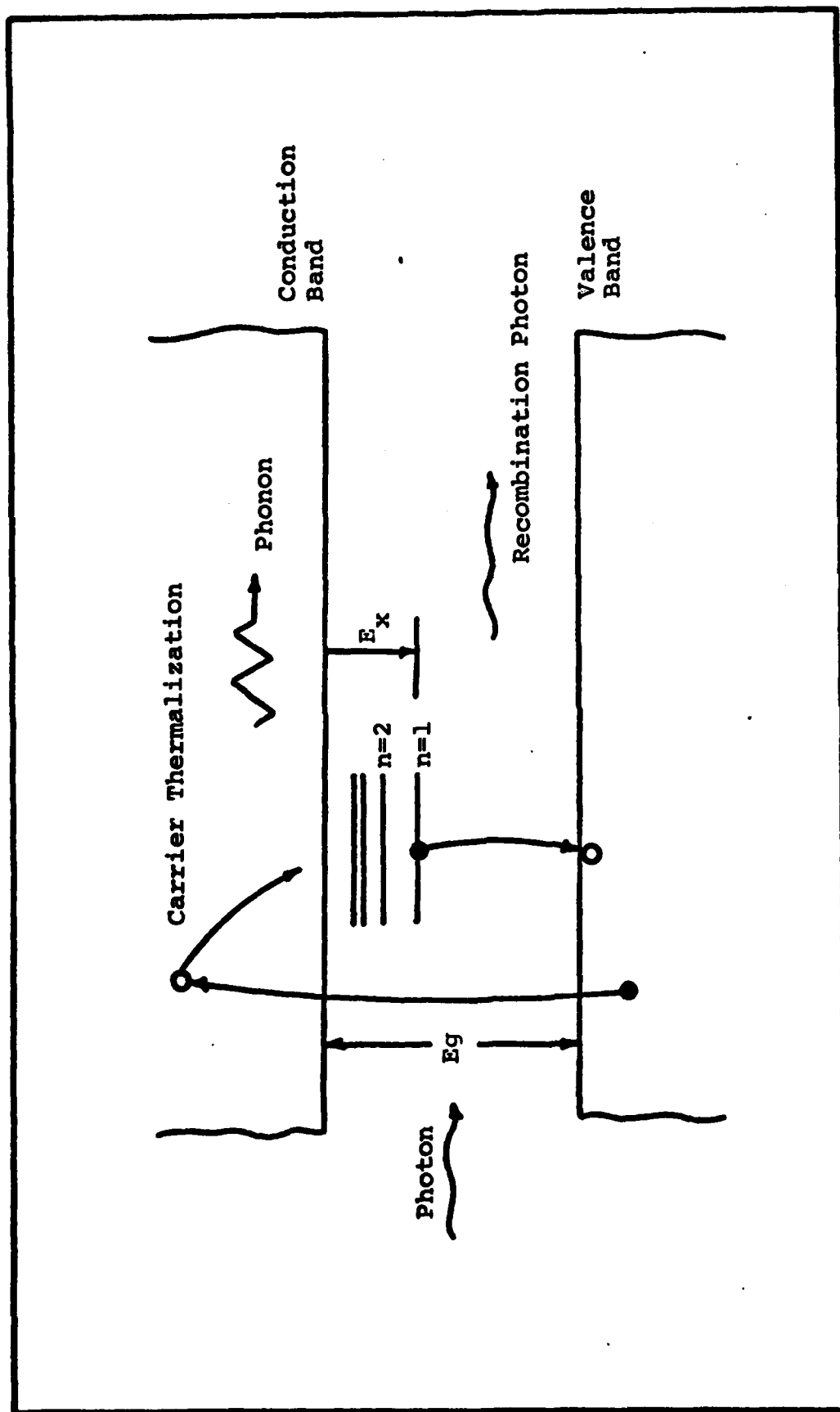


Figure 1: Exciton Formation (Wolfe, 1982)

### The Exciton-Plasma Mott Transition

Consider a free exciton (FE) gas and ask the question, "How can the bound electrons and holes become dissociated?"

One way in which the E-H pairs may become dissociated is through thermal ionization. This is a diffuse process in that, for a given temperature, the FE gas and EHP coexist in thermal equilibrium and there is not a precisely defined E-H pair density at which dissociation occurs.

Another way in which E-H pairs may become dissociated is through entropy ionization (see for example: Mock, 1978). This is a complicated effect which occurs when the total number of electrons and holes in the system is reduced at constant temperature. The important point here is again that there is no precisely defined E-H pair density at which dissociation occurs.

The third way in which excitons may ionize is through screening. In this case the exciton density is increased, at constant temperature, by increasing the optical pumping power and a point is reached at which a given electron can no longer be associated with any particular hole. Here there is a precisely defined density at which the excitonic binding energy goes to zero. The transition is from an insulating FE gas to a metallic electron-hole plasma (EHP) and is called a Mott transition.

Thus, the Mott transition is an insulator-to-metal transition which arises as a result of screening.

## II. Experiment

Experimentally, the exciton-plasma Mott transition has been studied in connection with a separate transition which is known to occur and which is well understood. This other transition is a first-order phase transition in which the FE gas condenses into a highly dense metallic electron-hole liquid (EHL). Experimental work may be seen for example in Hammond et al (Hammond, 1976), Thomas et al (Thomas, 1973), and Thomas et al (Thomas, 1974). A thorough discussion of the theory of the EHL is given by Rice (Rice, 1977).

The EHL is important in the experimental study of the Mott transition and will thus be briefly discussed.

The phase diagram for the electron-hole system is shown in Figure 2. How such a phase diagram is constructed will be discussed shortly. For the present it is sufficient to note that below a certain critical temperature,  $T_c$ , a two-phase region exists where the FE gas (or EHP) is in equilibrium with the dense EHL. The solid curve is the liquid-gas coexistence curve. If the FE gas density is increased (by increased optical pumping at sufficiently low, constant temperature), the gas-to-liquid transition will occur when the FE gas density reaches the value on the coexistence curve. The EHL will then be present in droplets whose density is determined by the liquid side of the coexistence curve. Further increases in optical pumping change the size of the electron-hole droplets but do not change their density.

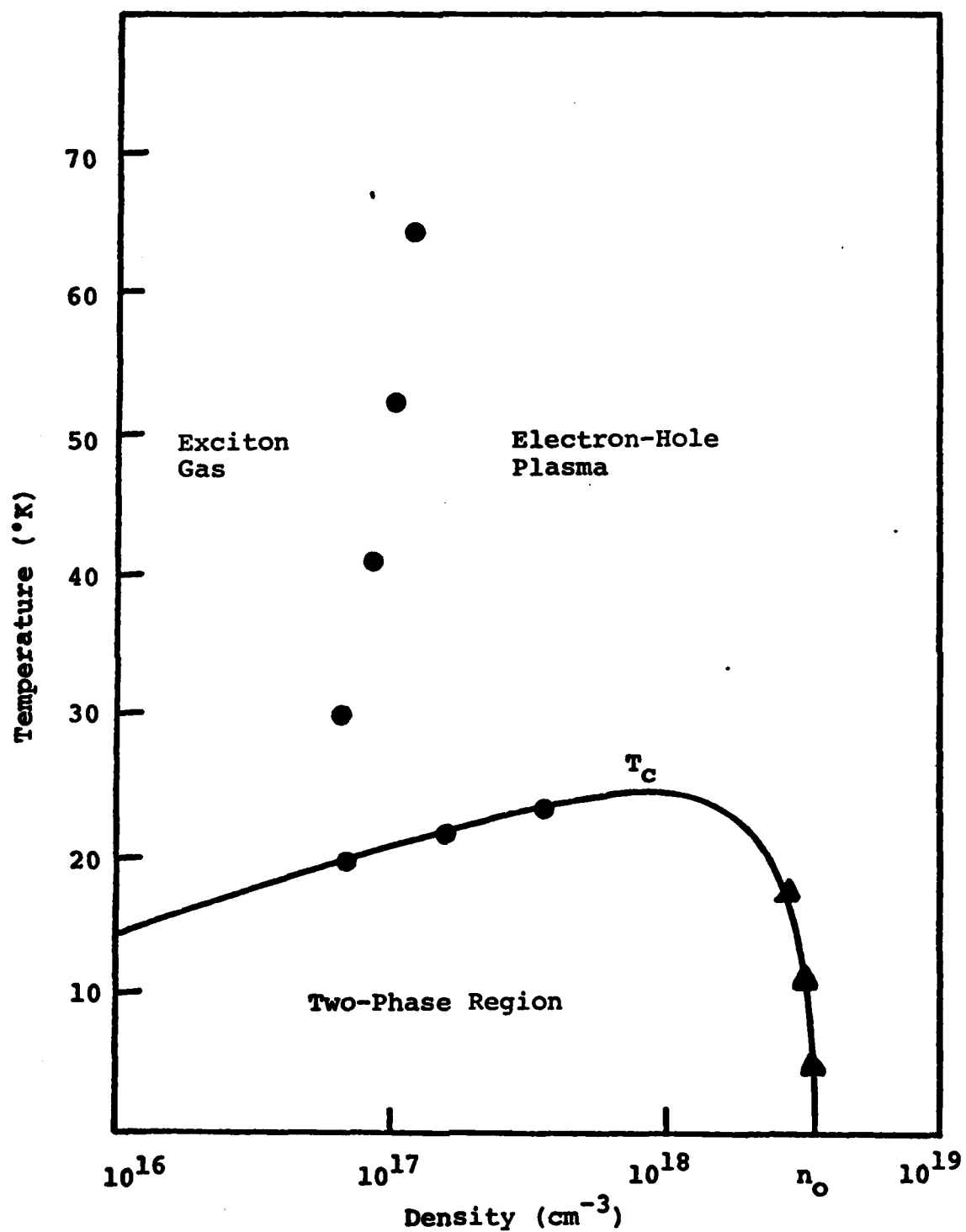


Figure 2: Phase Diagram



Given the above comments on the EHL, one may now turn to the experimental construction of the phase diagram of Figure 2. This construction will be illustrated through a discussion of a specific experimental study of the exciton-plasma Mott transition (Shah, 1977). Shah and his co-workers were first to report experimental evidence for the Mott dissociation of excitons into EHP. Their work shows clearly how the experimental data are obtained and interpreted. This discussion will thus serve to define the theoretical problem as well as to provide the experimental background.

#### The Luminescence Spectra

Shah and his co-workers excited a crystal of pure Si with radiation from an argon laser and observed the resulting luminescence spectra at various temperatures and for various optical pumping powers.

The spectra which they observed at low temperature (18°K) are shown in Figure 3. For low pumping powers, the FE line was seen, while for sufficiently high pumping powers, a second peak due to EHL luminescence was also present. Both of these luminescence peaks were found to have line shapes which were independent of pumping power.

Figure 4 shows the spectra which were obtained at 23°K. For low pumping power, the FE line was again seen. However, as the incident power was increased, the low energy side of the FE line was observed to broaden as shown by the singly dashed curve. Again, for sufficiently high pumping powers,

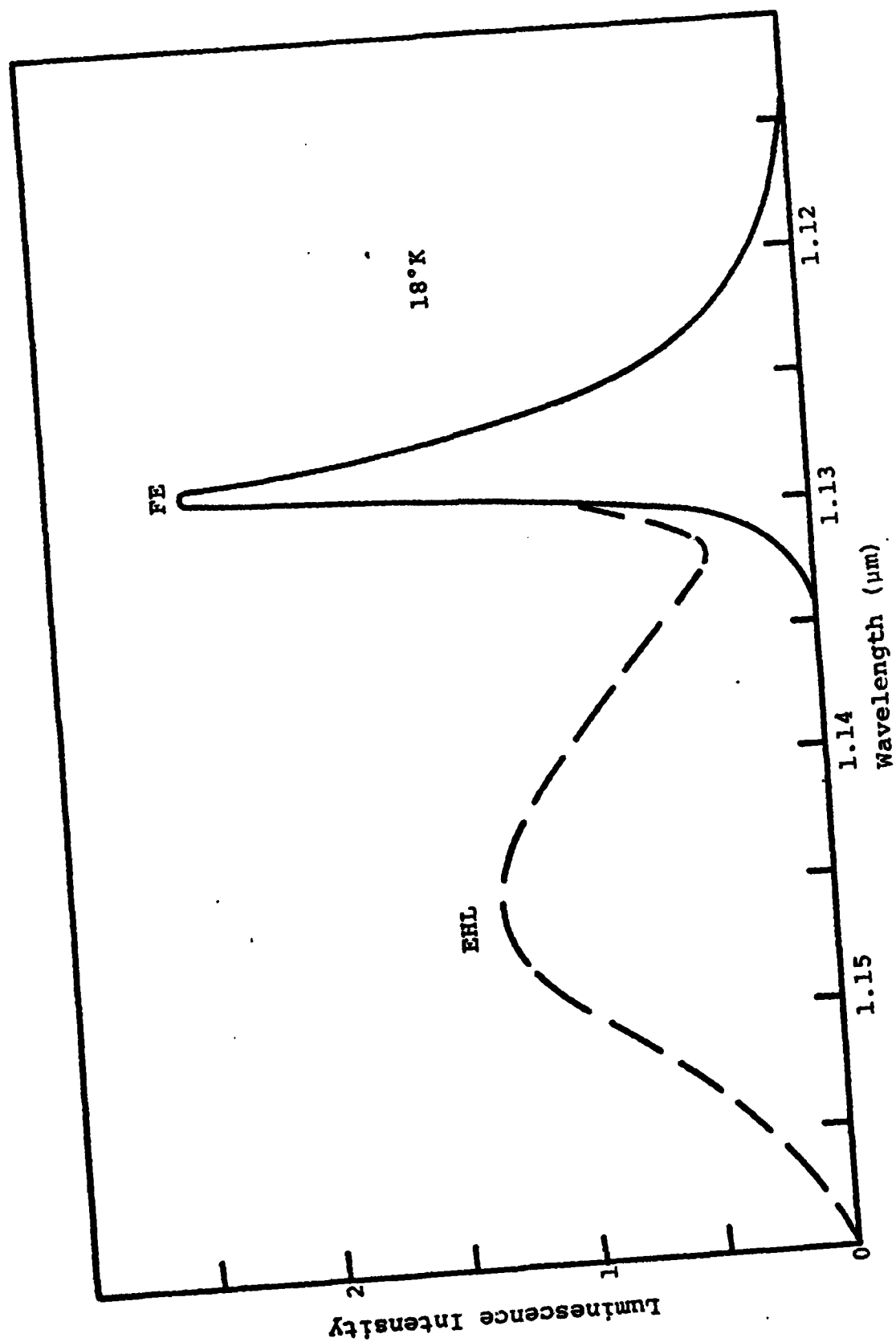


Figure 3: Luminescence Spectra (18°K) (Shah, 1977)

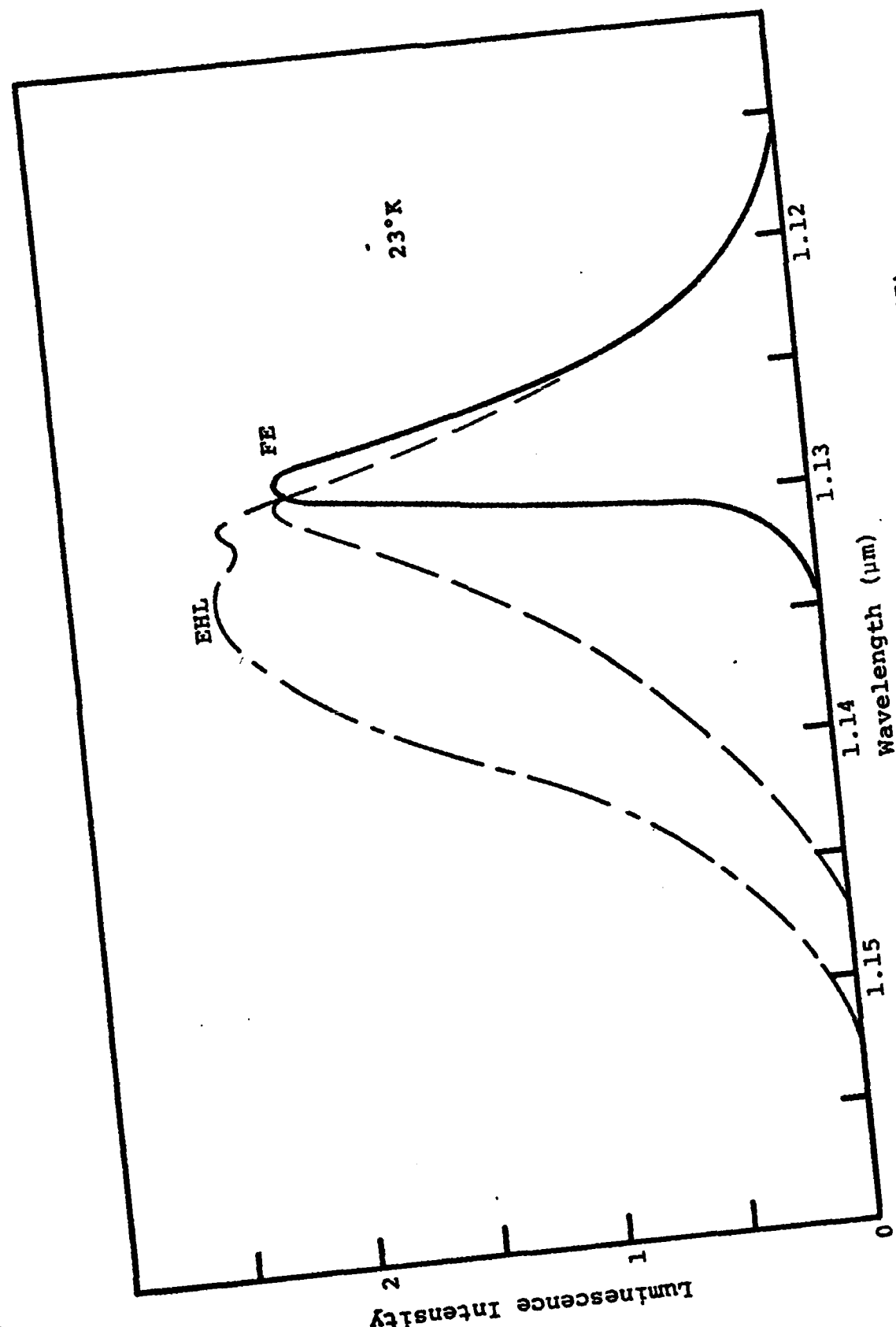


Figure 4: Luminescence Spectra (23°K) (Shah, 1977)

the second peak due to the formation of EHL was observed.

The spectra obtained at 30°K, which is above the critical temperature for the formation of an EHL, are shown in Figure 5. At low incident power the FE line was observed (curve 1), and as the power was increased, the line broadening was seen to evolve continuously into a shape which is well fit by a plasma line shape (curve 3).

Shah and his co-workers interpreted the observed line broadening as being due to the Mott dissociation of excitons into an EHP. This is a logical interpretation since the FE line shape is independent of pumping power, while the line shape due to the recombination of unbound electrons and holes does depend on pumping power. It is thus natural to associate the onset of the line broadening with the onset of the Mott dissociation. How this was quantified will now be presented.

#### The Threshold Pumping Powers

In order to determine the threshold powers for the Mott transition, and for the formation of EHL, Shah and his co-workers plotted the change in position of the low energy half-maximum of each distinct peak observed in the spectra. The change was plotted as a function of average incident power. The results are shown in Figure 6.

At 18°K, only the FE and EHL peaks were seen and their shapes were independent of pumping power. Thus the power,  $I_T$ , at which the EHL peak was first observed was taken as the threshold for EHL formation.

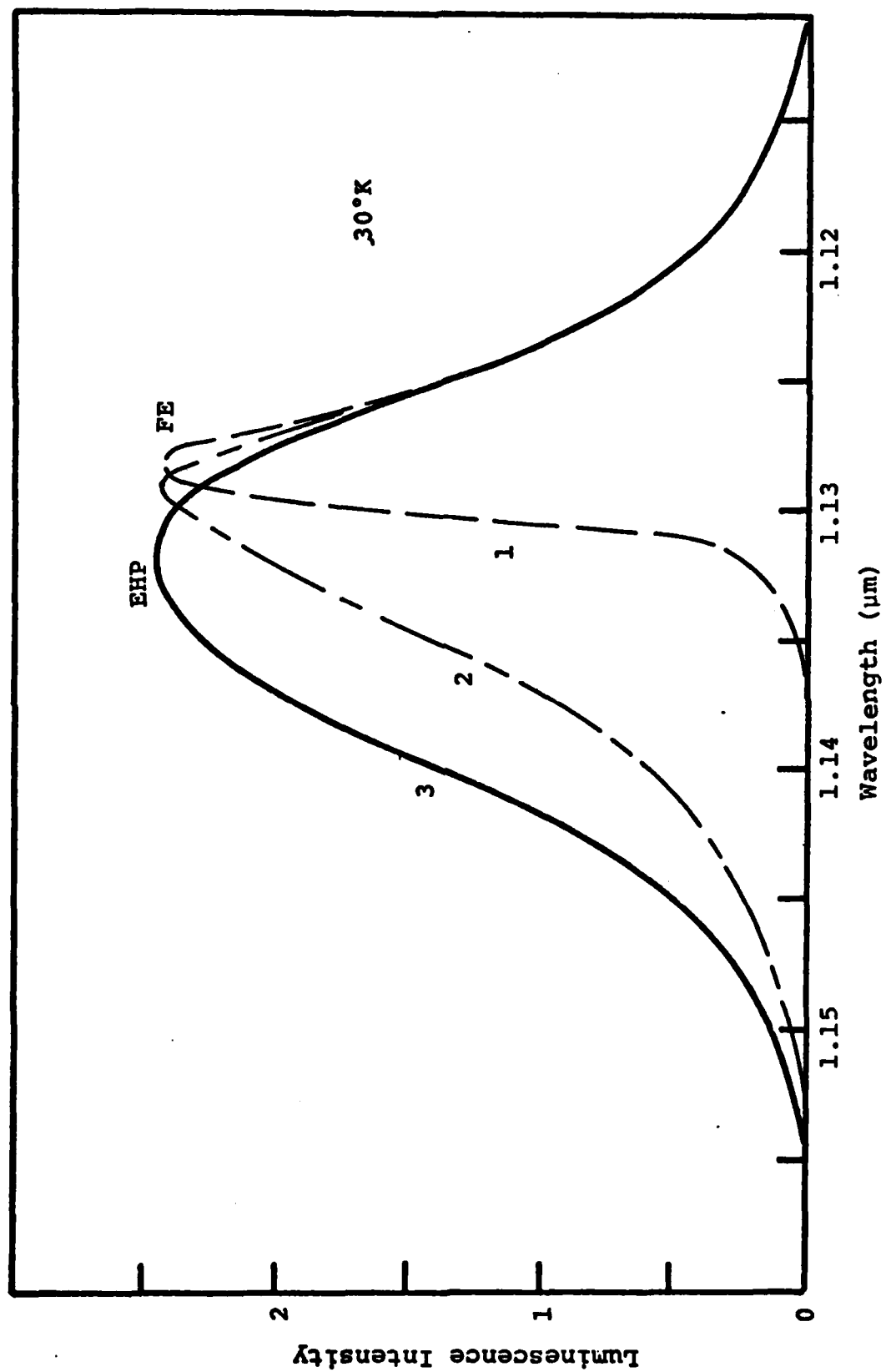


Figure 5: Luminescence Spectra (30°K) (Shah, 1977)

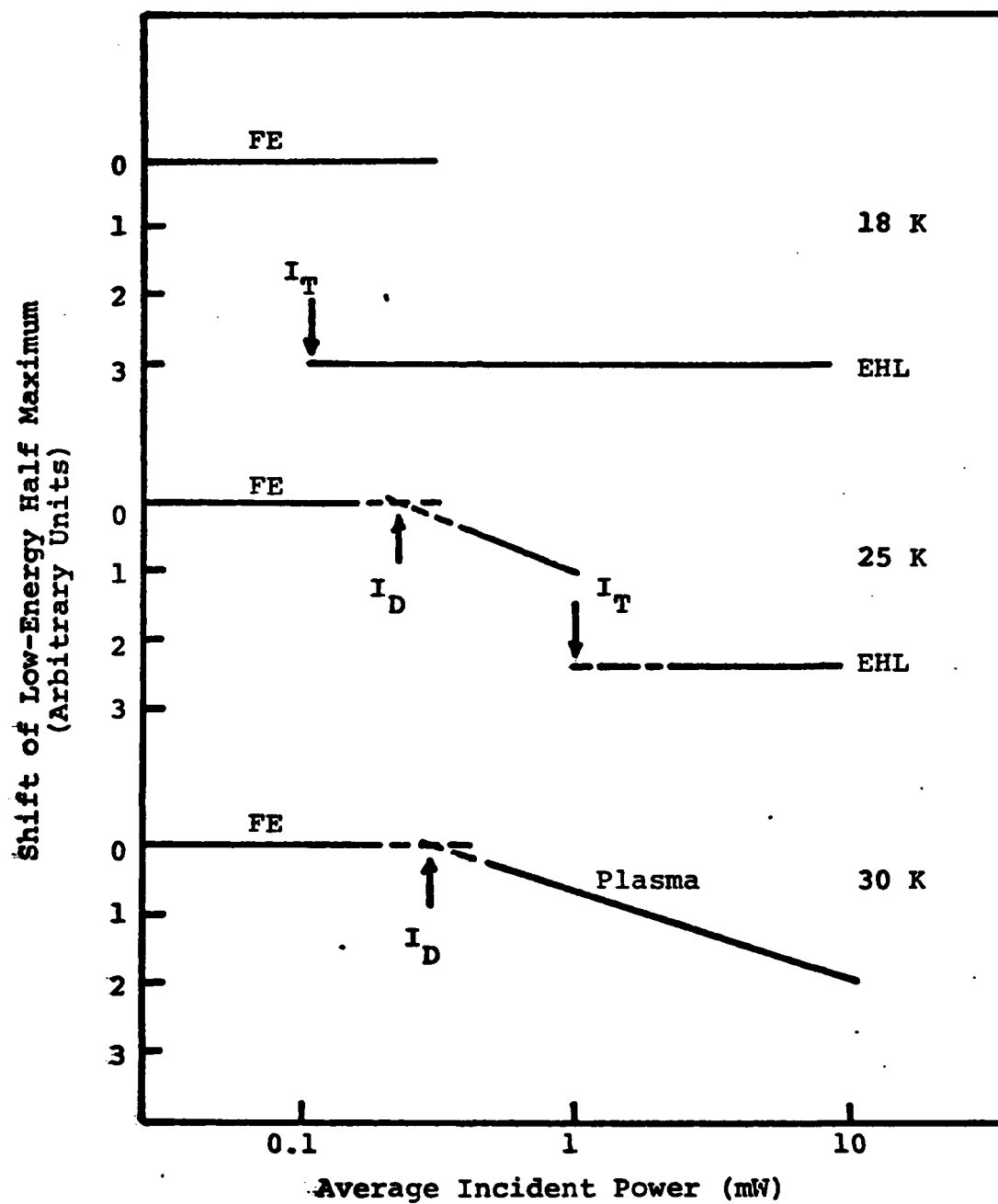


Figure 6: Determination of Threshold Powers (Shah, 1977)

At 25°K, the line broadening was found to yield a linear plot between the FE and EHL plots.  $I_T$  was determined as before for EHL condensation. The threshold,  $I_D$ , for the onset of line broadening was determined by extrapolation as shown.

At 30°K, the continuous broadening was observed and  $I_D$  was again determined by extrapolation.

Once the threshold powers were determined, there remained the problem of converting those powers into E-H pair densities. This problem was solved by constructing the phase diagram for the E-H system.

#### The Phase Diagram

The phase diagram for the E-H system in Si was shown in Figure 2. The solid curve is taken from Norris and Bajaj (Norris, 1982), while the circle and triangle points are included to aid in the description of how Shah et al constructed a similar phase diagram.

The EHL densities (triangular points) were determined from the liquid luminescence half-width by using the theoretical calculations of Hammond, McGill, and Mayer (Hammond, 1976). This process resulted in the experimental determination of  $n_0$ , the EHL density at 0°K.

Given experimental values for  $n_0$  and  $T_c$  (the critical temperature for EHL condensation) the theoretical calculations of Reinecke and Ying (Reinecke, 1975) were used to obtain the liquid-gas coexistence curve (solid line). It

was thus possible to determine the FE gas densities (circles on the solid curve) which were in equilibrium with the EHL at various temperatures, and to associate these densities with the measured threshold powers ( $I_T$ ) for EHL condensation.

The Mott transition densities were then determined from the threshold powers,  $I_D$ , by assuming a temperature-independent, linear scaling between E-H pair density and pumping power. This assumption is of uncertain validity but represents the best method available for the experimental determination of the Mott transition densities.

#### The Theoretical Problem

The above discussion clearly defines the theoretical problem for the Mott transition: One must predict the densities at which excitons become unbound due to screening. A theory for doing this will be discussed in the following chapter and will be extended to take conduction band anisotropy into account.



### III. Theory

As was mentioned in the introduction, Norris and Bajaj (Norris, 1982) have developed a theory for the exciton-plasma Mott transition in Si which is in good agreement with experiment. They obtained the exciton Hamiltonian by assuming isotropic masses and by assuming static electron-hole (E-H) screening in the random phase approximation (RPA). They then associated the Mott transition at a given temperature with the E-H pair density for which the binding energy of the exciton becomes zero. The binding energy was evaluated variationally. In this chapter, the above theory will be presented and extended to take into account the conduction band anisotropy. As was mentioned earlier, this is being done in order to assess the effects of the electron anisotropy on the exciton-plasma Mott transition both in Si and (more importantly) in Ge.

#### Background

Theoretical work on the exciton-plasma Mott transition was preceded by investigations of the similar problem of an electron bound to a donor impurity in a many-valley semiconductor. In the latter case, the task is to compute the donor concentration,  $N_c$ , at which the electrons become unbound due to screening. Since the theory to be presented in this work is a direct product of the earlier work, the donor impurity problem will now be reviewed.

Initially, the screening was taken into account by assuming the electron to be bound in a Yukawa potential, and the variational calculations were done using hydrogenic trial functions (Mott, 1949). Later, Rogers et al (Rogers, 1970) numerically integrated Schrödinger's equation for the above case. The two results were not in very good agreement, and hydrogenic wave functions were seen to be poor trial functions.

Later, Lam and Varshni (Lam, 1971) did the variational calculation for the Yukawa potential using eigenfunctions of the Hulthén potential. Their results were in good agreement with the calculation of Rogers. The Hulthén potential and its s-state eigenfunction, as given by Greene et al (Greene, 1977) are

$$V_H(\underline{r}) = - \frac{e^2 \mu e^{-\mu r}}{\epsilon_0 (1 - e^{-\mu r})} \quad (1)$$

and

$$\psi(\underline{r}) = \frac{1}{2(\pi a)^{3/2}} \left( \frac{4}{\mu^2} - 1 \right)^{1/2} \frac{e^{-(1 - \mu/2)r/a} - e^{-(1 + \mu/2)r/a}}{r} \quad (2)$$

where  $e$  is the electronic charge,  $\epsilon_0$  is the static dielectric constant,  $a$  is the first Bohr radius of the electron, and  $\mu$  is taken as a variational parameter. Greene et al used the Hulthén wave function to solve the problem of an electron in the Lindhard potential (RPA) at  $T = 0$  and of an electron in the Hubbard-Sham potential (which includes first order

corrections to the RPA at  $T = 0$ ). Their result for the Hubbard-Sham potential was in good agreement with the result of Martino et al (Martino, 1973), who solved the corresponding Schrödinger equation numerically. Thus the Hulthén wave function was again seen to be a good trial function.

In all of the above work, the electron masses were taken to be isotropic. Since the electron masses in many-valley semiconductors are anisotropic, Aldrich (Aldrich, 1977) treated the problem of an electron with anisotropic mass bound in the Lindhard and Hubbard-Sham potentials at  $T = 0$ . He performed the variational calculation using a modified form of the Hulthén wave function, which will be used in the present work:

$$\psi(\underline{r}) = \frac{1}{a^{3/2}} \left( \beta^{3/2} \frac{4-\mu^2}{4\pi\mu^2} \right)^{1/2} \frac{e^{-\rho/a} (e^{\mu\rho/2a} - e^{-\mu\rho/2a})}{\rho/a} \quad (3)$$

where  $a$  is the Bohr radius,  $\beta$  and  $\mu$  are variational parameters, and where  $\rho$  is given by:

$$\rho = \left[ \frac{m_\ell}{m^*} a_\ell x^2 + \frac{m_t}{m^*} a_t (y^2 + z^2) \right]^{1/2} \quad (4)$$

Ellipsoidal energy surfaces are assumed so that longitudinal and transverse masses,  $m_\ell$  and  $m_t$ , may be introduced, and  $m^* \equiv (m_\ell m_t^2)^{1/3}$ . The parameters  $a_\ell$  and  $a_t$  are given by

$$a_\ell = \beta \epsilon^{2/3} \quad (5a)$$

$$a_t = \beta/\epsilon^{1/3} \quad (5b)$$

where  $\epsilon$  is a third variational parameter. The variational parameter,  $\mu$ , reflects the strength of the Hulthén potential,  $\beta$  effectively expands or contracts the wave function, and  $\epsilon$  adjusts the trial function anisotropy.

The above discussion shows how the choice of RPA screening has come about and how the variational approach has developed. The theory of Norris and Bajaj for the exciton-plasma Mott transition will now be presented in detail via its extension to include electron anisotropy. This will be done by considering first the exciton Hamiltonian, and then the variational calculation for the excitonic binding energy.

#### The Exciton Hamiltonian

The exciton Hamiltonian is taken to be

$$H = -\frac{\hbar^2}{2} \sum_{i=1}^3 \left[ \frac{1}{m_{ei}} \frac{\partial^2}{\partial x_{ei}^2} + \frac{1}{m_{hi}} \frac{\partial^2}{\partial x_{hi}^2} \right] + U(\underline{r}_e - \underline{r}_h) \quad (6)$$

where  $1/m_{ei}$  and  $1/m_{hi}$  ( $i = 1, 2, 3$ ) are the diagonal elements of the electron and hole effective mass tensors. The position vectors for electrons and holes are  $\underline{r}_e$  and  $\underline{r}_h$ , while  $x_{ei}$  and  $x_{hi}$  are the components of these vectors.  $U(\underline{r}_e - \underline{r}_h)$  is the interaction potential.

In writing the kinetic energy term for the electron in equation (6), ellipsoidal energy surfaces have been

assumed. The hole mass will be taken to be isotropic: The effective mass tensor notation has been retained in the kinetic energy term for holes in order to make the derivations easier. The assumption of isotropic hole masses has been made because any attempt to go beyond this assumption would make the problem intractable. For a complete treatment of the hole kinetic energy see (Lipari, 1971), and for a discussion of semiconductor band structure see (Rice, 1977: page 5).

A center of mass transformation is now made in order to treat the e-h pair mathematically as a single particle in the assumed potential. Thus

$$\underline{r} \equiv \underline{r}_e - \underline{r}_h \quad (7a)$$

$$x_i \equiv \frac{m_{ei}x_{ei} + m_{hi}x_{hi}}{m_{ei} + m_{hi}} \quad (7b)$$

$$\frac{1}{m_i} \equiv \frac{1}{m_{ei}} + \frac{1}{m_{hi}} \quad (7c)$$

where the  $m_i$  are reduced masses. Ignoring the translational term, which does not affect the binding energy, one obtains

$$H = -\frac{\hbar^2}{2} \sum_{i=1}^3 \frac{1}{m_i} \frac{\partial^2}{\partial x_i^2} + U(\underline{r}) \quad (8)$$

Since the energy surfaces are assumed ellipsoidal, longitudinal and transverse effective masses may be introduced:

$$m_{e\ell} = m_{e1} , m_{et} = m_{e2} = m_{e3} \quad (9a)$$

$$m_{h\ell} = m_{h1} , m_{ht} = m_{h2} = m_{h3} \quad (9b)$$

It should again be noted that the hole masses are assumed to be isotropic and that the introduction of  $m_{h\ell}$  and  $m_{ht}$  is solely for ease of derivation.

The reduced masses are thus given by

$$\frac{1}{m_{\ell}} = \frac{1}{m_{e\ell}} + \frac{1}{m_{h\ell}} \quad (10a)$$

$$\frac{1}{m_t} = \frac{1}{m_{et}} + \frac{1}{m_{ht}} \quad (10b)$$

and the exciton Hamiltonian is given by

$$H = -\frac{\hbar^2}{2} \left[ \frac{1}{m_{\ell}} \frac{\partial^2}{\partial x^2} + \frac{1}{m_t} \left( \frac{\partial^2}{\partial y^2} + \frac{\partial^2}{\partial z^2} \right) \right] + U(\underline{r}) \quad (11)$$

In order to complete the determination of the Hamiltonian, an explicit expression for the potential energy must be obtained. This is done in wave-vector space (the Fourier transform domain of position space) by assuming static electron-hole screening in the random phase approximation. It is thus assumed that the electrons and holes respond to the unscreened (Coulomb) potential individually rather than collectively. It is thus also assumed that the total potential can be written as the unscreened potential plus

a term which represents the average response of the screening carriers to the total potential. For electron screening this is

$$V(\underline{r}) = V_0(\underline{r}) - \int \frac{e \langle \hat{n}_{\underline{r}'} \rangle}{|\underline{r} - \underline{r}'|} d^3 r' \quad (12)$$

where  $V(\underline{r})$  is the total potential at  $\underline{r}$ ,  $V_0(\underline{r})$  is the unscreened potential at  $\underline{r}$ , and  $\langle \hat{n}_{\underline{r}'} \rangle$  is the expected value of the screening particle density at  $\underline{r}'$ .

The particle density  $\langle \hat{n}_{\underline{r}'} \rangle$  is given by

$$\langle \hat{n}(\underline{r}) \rangle = \text{Trace}(\hat{\rho}[V] \hat{n}(\underline{r})) \quad (13)$$

where  $\hat{\rho}[V]$  is the density matrix and  $\hat{n}$  is the particle density operator. The density matrix is obtained from its equation of motion

$$- i\hbar \frac{\partial \hat{\rho}}{\partial t} = [\hat{\rho}, \hat{H}] \quad (14)$$

where  $\hat{H}$  is the system Hamiltonian. The density matrix and Hamiltonian are written in terms of perturbations:

$$\hat{\rho} = \hat{\rho}_0 + \delta \hat{\rho} \quad (15a)$$

$$H = H_0 + V \quad (15b)$$

The subscript "zero" refers to the problem in the absence of an external potential and  $V$  includes both the external and screening potentials. The RPA arises when equation (12) is assumed and the term in  $\delta \rho V$  is dropped from equation (14).

When the above analysis is carried out for both electrons and holes, the potential energy is found to be given by

$$V(\underline{q}) = - \frac{4\pi e^2}{\epsilon_0 q^2} \frac{1}{\epsilon(\underline{q})} \quad (16)$$

where  $e$  is the electronic charge,  $\epsilon_0$  is the static dielectric constant,  $\underline{q}$  is the wave-vector (of magnitude  $q$ ), and where  $\epsilon(\underline{q})$  is the dielectric function. The dielectric function is given by

$$\epsilon(\underline{q}) = 1 - \frac{4\pi e^2}{\epsilon_0 q^2} [v_e g_e(\underline{q}) + v_h g_h(\underline{q})] \quad (17)$$

where  $v_e$  and  $v_h$  are the band degeneracy factors for electrons and holes, and where the  $g$  functions are the density-density response functions for electrons and holes. The response function for electrons is

$$g_e(\underline{q}) = \frac{1}{8\pi^3} \int d^3k \frac{f[(E_e(\underline{k}) - \mu_e)/k_b T] - f[(E_e(\underline{k} - \underline{q}) - \mu_e)/k_b T]}{E_e(\underline{k}) - E_e(\underline{k} - \underline{q})} \quad (18)$$

with a similar expression for holes. In equation (18),  $d^3k$  is the wave-vector volume element  $dk_x dk_y dk_z$ ,  $f$  is the Fermi-Dirac function  $f(x) = 1/(e^x + 1)$ ,  $E_e$  is the energy as a function of wave-vector,  $\mu_e$  is the chemical potential for electrons, and  $k_b T$  is Boltzmann's constant times the absolute temperature.



Now, the integral in equation (18) has been evaluated for practical computation by Meyer (Meyer, unpublished), assuming spherical energy surfaces. In order to do the present work, it was therefore necessary to assume ellipsoidal energy surfaces according to

$$E_e(\underline{k}) = \frac{\hbar^2}{2m_{el}} k_x^2 + \frac{\hbar^2}{2m_{et}} (k_y^2 + k_z^2) \quad (19)$$

and cast the expression for the dielectric function into a form where Meyer's results could be used. The details of this process are outlined in the appendix. The result is

$$\epsilon(\underline{q}) = 1 + \frac{4\pi n e^2}{\epsilon_0 k_b T} \left[ \frac{F_{-\frac{1}{2}}(\eta_e)}{F_{\frac{1}{2}}(\eta_e)} G(x_{eo}, \eta_e) + \frac{F_{-\frac{1}{2}}(\eta_h)}{F_{\frac{1}{2}}(\eta_h)} G(x_{ho}, \eta_h) \right] \frac{1}{q^2} \quad (20)$$

where  $n$  is the electron-hole pair density, the  $\eta$ 's are the reduced Fermi energies (the chemical potentials divided by  $k_b T$ ), and where

$$G(x_o, \eta) = \frac{1}{(\pi x_o)^{\frac{1}{2}}} \frac{1}{F_{-\frac{1}{2}}(\eta)} \int_0^\infty f(x-\eta) \ln \left| \frac{1 + \frac{1}{2} \left( \frac{x_o}{x} \right)^{\frac{1}{2}}}{1 - \frac{1}{2} \left( \frac{x_o}{x} \right)^{\frac{1}{2}}} \right| dx \quad (21)$$

$$F_k(\eta) = \frac{1}{k!} \int_0^\infty x^k f(x - \eta) dx \quad (\text{Fermi integral; order } k) \quad (22)$$

and

$$x_{eo} = \frac{1}{2} \frac{\hbar^2}{m_e^* k_b T} \left[ \frac{m_e^*}{m_{el}} q_x^2 + \frac{m_e^*}{m_{et}} (q_y^2 + q_z^2) \right] \quad (23)$$

with a similar expression for  $x_{ho}$ . In equation (23)  $m_e^* \equiv (m_{el} m_{et}^2)^{1/3}$ . Again  $f$  is the Fermi-Dirac function. Meyer has cast the function  $G(x_o, \eta)$  into approximate analytical form and his results can (and will) be used in the present work provided equation (23) is used for  $x_{eo}$  along with the corresponding expression for  $x_{ho}$ .

The explicit expression for the potential energy term in the Hamiltonian has now been obtained (equation 16 combined with equation 20). The variational calculation for the exciton binding energy will now be presented.

### The Variational Calculation

It was mentioned at the beginning of this chapter, that the Mott transition at a given temperature is associated with the E-H pair density for which the exciton binding energy is zero. The binding energy is computed variationally by minimizing the expectation value of the Hamiltonian,  $\langle H \rangle$ , where  $\langle H \rangle$  is computed using the Hulthén wave function given in equation (3). This section will therefore address the determination of  $\langle H \rangle = \langle T \rangle + \langle V \rangle$ , where  $\langle T \rangle$  and  $\langle V \rangle$  are the expectation values of the kinetic and potential energies, and will conclude with a discussion of the minimization process.

The Kinetic Energy:  $\langle T \rangle$

As previously discussed, the trial function for the variational calculation is

$$\psi(\underline{r}) = \frac{2}{a^{3/2}} \left[ \beta^{3/2} \frac{4-\mu^2}{4\pi\mu^2} \right]^{1/2} \frac{e^{-\rho/a}}{\rho/a} \sinh\left(\frac{\mu\rho}{2a}\right) \quad (24)$$

where  $\rho$  is given by

$$\rho = \left[ \frac{m_\ell}{m^*} a_\ell x^2 + \frac{m_t}{m^*} a_t (y^2 + z^2) \right]^{1/2} \quad (25)$$

and where  $a = \epsilon_0 \hbar^2 / m^* e^2$  is the exciton Bohr radius. The masses  $m_\ell$  and  $m_t$  are the longitudinal and transverse reduced masses introduced in the discussion of the Hamiltonian, while  $m^* = (m_\ell m_t^2)^{1/3}$ . Also,  $a_\ell = \beta \epsilon^{2/3}$  and  $a_t = \beta / \epsilon^{1/3}$ , as previously defined. The variational parameters are  $\mu$ ,  $\beta$ , and  $\epsilon$ .

The expectation value for the kinetic energy,

$$\langle T \rangle = \int \psi^* \left\{ -\frac{\hbar^2}{2} \left[ \frac{1}{m_\ell} \frac{\partial^2}{\partial x^2} + \frac{1}{m_t} \left( \frac{\partial^2}{\partial y^2} + \frac{\partial^2}{\partial z^2} \right) \right] \right\} \psi d^3r \quad (26)$$

can be evaluated analytically. The result is

$$\langle T \rangle = \frac{H^*}{24} (a_\ell + 2a_t) (4 - \mu^2) \quad (27)$$

where  $H^* = m^* e^4 / \epsilon_0 \hbar^2$  is the reduced mass Hartree, the energy unit used in this work.

### The Potential Energy: $\langle V \rangle$

The potential energy can not be expressed in closed form in position space and its expectation value is, therefore, determined by a calculation in wave-vector space. In the usual expression for the expectation value for  $U(\underline{r})$ ,

$$\langle U \rangle = \int \psi^* U \psi d^3r \quad (28)$$

$U$  is expressed as the inverse Fourier transform of the potential,  $V(\underline{q})$ . Thus

$$\langle U \rangle = \int \psi^* \left\{ \frac{1}{(2\pi)^3} \int V(\underline{q}) e^{i\underline{q} \cdot \underline{r}} d^3q \right\} \psi d^3r \quad (29)$$

where  $V(\underline{q})$  is the statically screened Coulomb potential given by equations (16) and (20).

It will be seen later that the determination of  $\langle U \rangle$  involves the numerical evaluation of a double integral on the unit square. It turns out that if the potential,  $V(\underline{q})$ , is used "as is" in equation (29), then the integrand will have a finite value on the side of the unit square which corresponds to infinite wave-vector magnitude. This difficulty can be eliminated if  $V(\underline{q})$  is expressed as the sum of a "screening" term and a Coulomb term. In this case, the expectation for the Coulomb term can be evaluated analytically, while the integration for the screening term involves an integrand which vanishes on the previously mentioned side of the unit square.

Thus one writes

$$V(\underline{q}) = - \frac{4\pi e^2}{\epsilon_0 q^2 \epsilon(\underline{q})} = V_s(\underline{q}) + V_c(\underline{q}) \quad (30)$$

where

$$V_s(\underline{q}) \equiv - \frac{4\pi e^2}{\epsilon_0 q^2} \left[ \frac{1 - \epsilon(\underline{q})}{\epsilon(\underline{q})} \right] \quad (31)$$

and

$$V_c(\underline{q}) \equiv - \frac{4\pi e^2}{\epsilon_0 q^2} \quad (32)$$

and where  $\epsilon(\underline{q})$  is the dielectric function.

When equation (30) is substituted into equation (29) for  $\langle U \rangle$ , two integrals result.

The Coulomb integral is found to be given by

$$\langle U_c \rangle = H^* \beta^{\frac{3}{2}} g(\mu) h(\epsilon) \quad (33)$$

where  $H^*$  is the Hartree, where  $\mu$ ,  $\beta$ , and  $\epsilon$  are the variational parameters in the trial wave function, and where the functions  $g(\mu)$  and  $h(\epsilon)$  are given by

$$g(\mu) = \frac{4 - \mu^2}{\mu^2} \ln \left[ \frac{4 - \mu^2}{4} \right] \quad (34a)$$

and

$$h(\epsilon) = \begin{cases} \left( \frac{m_t}{\epsilon m_\ell} \right)^{1/6} \left( 1 - \frac{m_t}{\epsilon m_\ell} \right)^{-1/2} \sin^{-1} \left[ \left( 1 - \frac{m_t}{\epsilon m_\ell} \right)^{1/2} \right] & , \frac{m_t}{\epsilon m_\ell} < 1 \\ \left( \frac{m_t}{\epsilon m_\ell} \right)^{1/6} \left( \frac{m_t}{\epsilon m_\ell} - 1 \right)^{-1/2} \ln \left[ \left( \frac{m_t}{\epsilon m_\ell} \right)^{1/2} + \left( \frac{m_t}{\epsilon m_\ell} - 1 \right)^{1/2} \right] & , \frac{m_t}{\epsilon m_\ell} > 1 \end{cases} \quad (34b)$$

For the screening term, one has

$$\langle U_{scr} \rangle = \int \psi^* \psi \left\{ \frac{1}{(2\pi)^3} \right\} V_s(\underline{q}) e^{i\underline{q} \cdot \underline{r}} d^3q \quad (35)$$

Now,  $\langle U_{scr} \rangle$  can be expressed as a single triple integration in  $q$ -space by making the change of variables from  $\underline{q}$  to  $-\underline{q}$  and interchanging the order of integration. One then obtains the integral over all  $q$ -space of  $V_s(\underline{q})$  times the Fourier transform of the wave function squared:

$$\langle U_{scr} \rangle = \frac{1}{(2\pi)^3} \int F(\psi^2) V_s(\underline{q}) d^3q \quad (36)$$

The Fourier transform,  $F$ , is easy to compute and is given by

$$F = \frac{4-\mu^2}{\mu^2} \frac{1}{aq} \left\{ \tan^{-1} \left( \frac{aq'}{2-\mu} \right) + \tan^{-1} \left( \frac{aq'}{2+\mu} \right) - 2 \tan^{-1} \left( \frac{aq'}{2} \right) \right\} \quad (37a)$$

where

$$q' \equiv \left[ \frac{m^*}{m_\ell a_\ell} q_x^2 + \frac{m^*}{m_t a_t} (q_y^2 + q_z^2) \right]^{\frac{1}{2}} \quad (37b)$$

The masses which appear in equation (37b) are the reduced masses,  $a$  is the Bohr radius, and the quantities  $a_\ell$  and  $a_t$  were defined in the section where the wave function was introduced (see equations 3-5).

The integral in equation (36) is evaluated after several changes of variables.

First, the spherical coordinates  $(q, \theta, \phi)$  defined below are introduced.

$$q_x = q \cos \theta \quad (38a)$$

$$q_y = q \sin \theta \cos \phi \quad (38b)$$

$$q_z = q \sin \theta \sin \phi \quad (38c)$$

The integration with respect to  $\phi$  can be done immediately, and one is left with a double integral. However, because of the complicated nature of the integrand, neither the  $q$ - nor the  $\theta$ -integration can be performed analytically and the double integral must be computed numerically.

The second and third changes of variables in equation (36) are to introduce respectively  $\tilde{q} = aq$  and  $u = \cos \theta$ . Again,  $a$  is the Bohr radius, and the "tilde" is used on  $q$  to indicate that  $\tilde{q}$  is a dimensionless wave-vector magnitude.

Thus, if the expression for  $V_s(q)$  in terms of the dielectric function (see equation (31)) is substituted into equation (36), one obtains

$$\langle U_{scr} \rangle = \frac{2}{\pi} H^* \int_0^1 du \int_0^\infty d\tilde{q} \left\{ F_3(u, \tilde{q}) \frac{\epsilon_3(u, \tilde{q}) - 1}{\epsilon_3(u, \tilde{q})} \right\} \quad (39)$$

The explicit expressions for  $F_3$  and  $\epsilon_3$  are complicated and will be presented after one final change of variables. Also, subscripts are used on  $F$  and  $\epsilon$  to denote the slightly different functions which come about because of the changes of variables. The subscript, 3, in equation (39) indicates the third change of variables.

The final change of variables is

$$s = \frac{\tilde{q}}{q_c + \tilde{q}} \quad (40)$$

which transforms the integral with respect to  $\tilde{q}$  into an integration on the interval  $0 \leq s \leq 1$ . One now obtains

$$\langle U_{scr} \rangle = \frac{2}{\pi} H^* \int_0^1 du \int_0^1 ds \left\{ \frac{q_c}{(1-s)^2} F_4(u, s) \frac{\epsilon_4(u, s) - 1}{\epsilon_4(u, s)} \right\} \quad (41)$$

The explicit forms for  $F_3$  and  $\epsilon_3$  are given below, while the explicit forms for  $F_4$  and  $\epsilon_4$  are obtained from those for  $F_3$  and  $\epsilon_3$  by replacing  $\tilde{q}$  by

$$\tilde{q} = q_c \frac{s}{1-s} \quad (42)$$



One has

$$F_3(u, \tilde{q}) = \left( \frac{4}{\mu^2} - 1 \right) \frac{1}{\tilde{q}'} \left\{ \tan^{-1} \left( \frac{\tilde{q}'}{2-\mu} \right) + \tan^{-1} \left( \frac{\tilde{q}'}{2+\mu} \right) - 2 \tan^{-1} \left( \frac{\tilde{q}'}{2} \right) \right\} \quad (43a)$$

with

$$\tilde{q}' = \frac{1}{\beta^{1/2}} \left( \frac{\epsilon m_\ell}{m_t} \right)^{1/6} \left[ 1 - \left( 1 - \frac{m_t}{\epsilon m_\ell} \right) u^2 \right]^{1/2} \tilde{q} \quad (43b)$$

and

$$\epsilon_3(u, \tilde{q}) = 1 + 4\pi (na^3) \frac{H^*}{k_b T} \left\{ \frac{F_{-1/2}(\eta_e)}{F_{1/2}(\eta_e)} G(x_{eo}, \eta_e) + \frac{F_{-1/2}(\eta_h)}{F_{1/2}(\eta_h)} G(x_{ho}, \eta_h) \right\} \frac{1}{\tilde{q}^2} \quad (44a)$$

with

$$x_{eo} = \frac{1}{2} \frac{m^*}{m_e} \frac{H^*}{k_b T} \left( \frac{m_{el}}{m_{et}} \right)^{1/3} \left[ 1 - \left( 1 - \frac{m_{et}}{m_{el}} \right) u^2 \right] \tilde{q}^2 \quad (44b)$$

and

$$x_{ho} = \frac{1}{2} \frac{m^*}{m_h} \frac{H^*}{k_b T} \left( \frac{m_{hl}}{m_{ht}} \right)^{1/3} \left[ 1 - \left( 1 - \frac{m_{ht}}{m_{hl}} \right) u^2 \right] \tilde{q}^2 \quad (44c)$$

As introduced in equation (22), the fractionally-subscripted F functions are Fermi integrals, and the G function is the integral which is evaluated by Meyer's interpolation.

It should be noted that all quantities in equations (43) and (44) have been put into forms where units cancel.

The quantity  $(na^3)$  may be identified as a dimensionless electron-hole pair density,  $H^*/k_b T$  may be defined as a dimensionless reciprocal temperature, and the quantities

$$\frac{m^*}{m_e} \frac{H^*}{k_b T} \text{ and } \frac{m^*}{m_h} \frac{H^*}{k_b T}$$

may be defined as dimensionless electron and hole reciprocal temperatures, respectively.

#### Minimization of the Total Energy

The routine used to find the binding energy,  $\langle H \rangle$ , (Shankland, private communication) minimizes a function of a given number of parameters. In this case,  $\langle H \rangle$  is a function of  $\mu$ ,  $\beta$ , and  $\epsilon$ , the parameters in the trial wave function introduced in Chapter III. The search for the minimum involves random, gradient, average, and jump steps, which are made initially with user defined frequencies, and finally, with frequencies generated in the course of the calculation. As convergence is obtained, the step size is automatically reduced to insure that the minimum is found. Finally, jump steps are made to allow for the possibility of local minima.

There are two possible approaches which can be taken to find the Mott transition density,  $n_{\text{Mott}}$ . One is to keep the electron-hole pair density as an input parameter and minimize  $\langle H \rangle$  as a function of  $\mu$ ,  $\beta$ , and  $\epsilon$ . The density is then adjusted manually until that density is found for which  $\langle H \rangle_{\text{minimized}} = 0$ . The other approach is to include the

density as a variational parameter in the minimization routine and minimize  $\langle H \rangle^2$ . The first approach has been adopted here because it is then easier to monitor the course of the calculation.

The procedure is to make a series of short calls (25 function evaluations each) to the minimization routine, looking for negative values of  $\langle H \rangle$ . Since the goal is to find the density for which  $\langle H \rangle_{\text{minimized}}$  is zero, and since the Mott transition is due to screening, one knows, as soon as a negative energy is obtained, that the density must be increased. The short calls, however, do not allow for the search step size to be reduced below about  $10^{-1}$  so that this initial search is a rough one. Once a series of positive energies is obtained, than a long call (250 function evaluations) is made to check for the best minimum. In this way the step size is reduced to about  $10^{-4}$ .

Results will now be presented for Si and Ge.

#### IV. Results

The material parameters used in this work are given in Table I (See Rice, 1977: page 8). Masses are given in units of the electron free-space mass. The longitudinal and transverse electron masses are given for Si and Ge. The electron masses used in the isotropic approximation are obtained from the optical mass average

$$m_{eo} \equiv 3 \left( \frac{2}{m_{et}} + \frac{1}{m_{el}} \right)^{-1} \quad (45)$$

while the hole masses,  $m_{hl}$  and  $m_{ht}$ , are the reciprocal of the Dresselhaus-Kip-Kittel A parameter given by Rice. The density of states masses,  $m_{edos}$  and  $m_{hdos}$ , are used in the calculation for the reduced Fermi energies and are determined from the following equations:

$$m_{edos} \equiv (m_{el} m_{et}^2)^{1/3} \quad (46a)$$

$$m_{hdos} \equiv \left( \frac{m_{hH}^{3/2} + m_{hL}^{3/2}}{2} \right)^{2/3} \quad (46b)$$

The equation for the hole density of states mass involves the heavy and light hole masses,  $m_{hH}$  and  $m_{hL}$ , and thus takes into account the fact that the heavy and light hole bands have been replaced by a single doubly-degenerate band. Table I also gives the static dielectric constant ( $\epsilon_0$ ) and the degeneracy factors ( $v_e, v_h$ ) for Si and Ge.

Table I: Material Parameters

	Si	Si (isotropic)	Ge	Ge (isotropic)
$m_{el}$	.9163	.2588	1.58	.1199
$m_{et}$	.1905	.2588	0.082	.1199
$m_{hl}$	.2336	.2336	.07474	.07474
$m_{ht}$	.2336	.2336	.07474	.07474
$m_{edos}$	.3216	.3216	.2198	.2198
$m_{hdos}$	.3637	.3637	.2247	.2247
$\epsilon_o$	11.4	11.4	15.36	15.36
$v_e$	6	6	4	4
$v_h$	2	2	2	2

The results obtained for the Mott transition in Si are shown in Table II. The Mott transition densities are given as a function of temperature with lower and upper bounds specified. Thus, for example, at  $T = 30^\circ K$

$$7.8 \times 10^{16} \text{cm}^{-3} < n_{\text{Mott}} < 8.0 \times 10^{16} \text{cm}^{-3} \text{ -- anisotropic Si}$$

$$7.4 \times 10^{16} \text{cm}^{-3} < n_{\text{Mott}} < 7.5 \times 10^{16} \text{cm}^{-3} \text{ -- isotropic Si}$$

The results of Table I for isotropic Si are in good agreement with the results of Norris and Bajaj (Norris, 1982).

Only two points have been determined for anisotropic Si

Table II: Mott Transition in Si

DENSITY ( $\times 10^{16} \text{cm}^{-3}$ )				
Si - ISOTROPIC			Si - ANISOTROPIC	
T(°K)	Lower Bound	Upper Bound	Lower Bound	Upper Bound
$10^{-4}$	3.7	3.8		
7.81	4.0	4.1	4.1	4.3
15.6	5.1	5.2		
23.4	6.3	6.4		
30.0	7.4	7.5	7.8	8.0
46.9	10.1	10.2		
62.5	12.7	12.8		
78.1	15.2	15.3		

since two points are sufficient to show the effects of conduction band anisotropy. It is seen that the Mott transition shifts to higher densities. The shift is 4% at  $T = 7.81^\circ\text{K}$  and 6% at  $T = 30.0^\circ\text{K}$ . These results will be interpreted after the results for Ge are presented.

The results for Ge are shown in Table III. Again, the Mott transition shifts to higher densities when conduction band anisotropy is taken into account. Here there is no apparent shift at  $5^\circ\text{K}$  while the shift at the higher temperatures is approximately 7%.

The observations which are to be made here are as follows: (1) The electron anisotropy causes the Mott

Table III. Mott Transition in Ge

T(°K)	DENSITY ( $\times 10^{16} \text{cm}^{-3}$ )			
	Ge - ISOTROPIC		Ge - ANISOTROPIC	
	Lower Bound	Upper Bound	Lower Bound	Upper Bound
5.0	.13	.15	.13	.15
12.5	.26	.27	.28	.29
20.0	.39	.395	.41	.43

transition to shift to higher densities. (2) The shift is greater for high temperatures than for low temperatures.

(3) The shift appears to be no greater in Ge than in Si.

The first observation can be explained by the fact that the anisotropy will reduce the ability of the electrons to screen and thus a higher density will be required to screen out the Coulomb potential. The second observation can be partially explained by noting that the electrons and holes have more thermal energy at higher temperatures and energetic carriers do not screen as effectively as less energetic carriers. The third observation is partially explained by a calculation of the exciton binding energy in the absence of screening.

Table IV shows binding energies in Ge for an electron bound to a hole and to a donor impurity, in the absence of screening. It can be seen that the anisotropy does not significantly affect the exciton binding energy. This is

Table IV: Binding Energies for Zero Screening (Ge)

Exciton	Binding Energy (meV)
Isotropic Masses	2.67
Anisotropic Masses	2.73
Donor Impurity	
Isotropic Masses	6.91
Anisotropic Masses	9.78

because the reduced masses are dominated by the light masses and in Ge one has  $m_{et} = .082$  and  $m_{hl} = m_{ht} = .075$ . Thus the ratio of longitudinal to transverse reduced mass is on the order of only two for the exciton. For the donor impurity, the above situation no longer prevails and the anisotropy significantly affects the binding energy. The result of 9.78 meV is in good agreement with Faulkner (Faulkner, 1969) who obtained 9.81 meV for an electron bound to a donor impurity in Ge.

Thus, the shift of the Mott transition densities is due mainly to the effects of the anisotropy on the screening since the anisotropy does not significantly affect the exciton binding energy.



## V. Summary and Conclusions

In this work, conduction band anisotropy has been incorporated into the theory of the exciton-plasma Mott transition (Norris, 1982). The exciton was treated mathematically as a particle in a screened Coulomb potential where static electron-hole screening in the random phase approximation was assumed. The Mott transition was associated with the electron-hole pair density at which the exciton binding energy in the assumed potential is zero, and the binding energy was computed variationally using the ground state eigenfunction of the Hulthén potential as a trial function.

The results obtained from the above theory lead to the following conclusions:

- (1) The conduction band anisotropy does not significantly affect the exciton binding energy.
- (2) The conduction band anisotropy decreases the ability of the electrons to screen and thus increases the Mott transition densities beyond those predicted by RPA screening with the conduction band taken as isotropic.
- (3) The effects of the electron anisotropy are no more pronounced in Ge than in Si.

## Bibliography

- Aldrich, C. "Screened Donor Impurities in Many-Valley Semiconductors with Anisotropic Masses," Physical Review B, 16: 2723 (1977).
- Faulkner, R. A. "Higher Donor Excited States for Prolate-Spheroid Conduction Bands: A Reevaluation of Silicon and Germanium," Physical Review, 3: 713 (1969).
- Forchel, A., B. Laurich, J. Wagner, and W. Schmid. "Systematics of Electron-Hole Liquid Condensation from Studies of Silicon with Varying Uniaxial Stress," Physical Review B, 25: 2730 (1982).
- Forchel, (to be published). Phys. Inst. Teil 4, Universitat, D 7-Stuttgart-80, Pfaffenwaldring 57, Germany.
- Greene, R. L., C. Aldrich, and K. K. Bajaj. "Mott Transition in Many-Valley Semiconductors," Physical Review B, 15: 2217 (1977).
- Hammond, R. B., T. C. McGill, and J. W. Mayer. "Temperature Dependence of the Electron-Hole-Liquid Luminescence in Si," Physical Review B, 13: 3566 (1976).
- Lam and Varshni. "Energies of s-Eigenstates in a Static Screened Coulomb Potential," Physical Review A, 4: 1875 (1971).
- Lipari, N. O. and A. Baldereschi. "Energy Levels of Indirect Excitons in Semiconductors with Degenerate Bands," Physical Review B, 15: 2497 (1971).
- Martino et al. "Metal to Non-Metal Transition in n-Type Many-Valley Semiconductors," Physical Review B, 8: 6030 (1973).
- Meyer, J. R. "Analytic Approximation of the Lindhard Dielectric Constant  $\epsilon(q, = 0)$  for Arbitrary Degeneracy," (unpublished) 1977.
- Mock, J. B., G. A. Thomas, and M. Combescot. "Entropy Ionization of an Exciton Gas," Solid State Communications, 25: 279 (1978).
- Mott, N. F. "The Basis of the Electron-Theory of Metals with Special Reference to the Transition Metals," Proceedings of the Physical Society of London, 62: 416 (1949).

Norris, G. B. and K. K. Bajaj. "Exciton-Plasma Mott Transition in Si," Physical Review B, 26: (to be published) (1982).

Reinecke and Ying. "Model of Electron-Hole Droplet Condensation in Semiconductors," Physical Review Letters, 35: 311 (1975).

Rice, T. M. "The Electron-Hole Liquid in Semiconductors: Theoretical Aspects," Solid State Physics: Advances in Research and Applications, edited by H. Ehrenreich, F. Seitz, and D. Turnbull (Volume 32). New York: Academic Press, 1977.

Rogers, F. J., H. C. Graboske Jr, and D. J. Harwood. "Bound Eigenstates of the Static Screened Coulomb Potential," Physical Review A, 1: 1577-1586 (1970).

Shah, J., M. Combescot, and A. H. Dayem. "Investigation of Exciton-Plasma Mott Transition in Si," Physical Review Letters, 38: 1497-1500 (1977).

Shankland, D., Professor, Department of Physics, Air Force Institute of Technology, Wright-Patterson Air Force Base, AFIT/ENP, WPAFB, OH 45433.

Thomas, G. A., T. G. Phillips, T. M. Rice, and J. C. Hensel. "Temperature-Dependent Luminescence from the Electron-Hole Liquid in Ge," Physical Review Letters, 31: 386-389 (1973).

-----, T. M. Rice, and J. C. Hensel. "Liquid-Gas Phase Diagram of an Electron-Hole Fluid," Physical Review Letters, 33: 219-222 (1974).

Wolfe, J. P. "Thermodynamics of Excitons in Semiconductors," Physics Today, March 1982.

### Appendix: The Anisotropic Dielectric Function

The screened Coulomb potential in wave-vector space is given by

$$V(\underline{q}) = - \frac{4\pi e^2}{\epsilon_0 q^2 \epsilon(\underline{q})} \quad (16)$$

where  $e$  is the electronic charge,  $\epsilon_0$  is the static dielectric constant,  $q$  is the wave-vector magnitude, and  $\epsilon(\underline{q})$  is the Lindhard dielectric function.

The dielectric function is given by

$$\epsilon(\underline{q}) = 1 - \frac{4\pi e^2}{\epsilon_0 q^2} [v_e g_e(\underline{q}) + v_h g_h(\underline{q})] \quad (17)$$

where  $v_e$  and  $v_h$  are the degeneracy factors and where  $g_e(\underline{q})$  and  $g_h(\underline{q})$  are the density-density response functions for electrons and holes respectively. The response function for electrons is given by

$$g_e(\underline{q}) = \frac{1}{8\pi^3} \int d^3k \left\{ \frac{f[(E_e(\underline{k}) - \mu_e)/k_b T] - f[(E_e(\underline{k}-\underline{q}) - \mu_e)/k_b T]}{E_e(\underline{k}) - E_e(\underline{k}-\underline{q})} \right\} \quad (18)$$

In equation (18),  $\mu_e$  is the chemical potential for electrons and  $f(x) = 1/(e^x + 1)$ , the Fermi-Dirac function. The function,  $E_e(\underline{k})$ , is defined by

$$E_e(\underline{k}) = \frac{\hbar^2}{2m_{el}} k_x^2 + \frac{\hbar^2}{2m_{et}} (k_y^2 + k_z^2) \quad (19)$$

where  $m_{el}$  and  $m_{et}$  are the longitudinal and transverse electron effective masses.

The explicit expression for the dielectric function is obtained by performing the integration in equation (18), with an almost identical calculation for holes. The first step is to make the following changes of variables in order to make  $E_e(\underline{k})$  and  $E_e(\underline{k}-\underline{q})$  spherically symmetric (Aldrich, 1977: 2724):

$$k_x = \left( \frac{m_{el}}{m_e^*} \right)^{1/2} s_x \quad q_x = \left( \frac{m_{el}}{m_e^*} \right)^{1/2} t_x \quad (A-1a)$$

$$k_y = \left( \frac{m_{et}}{m_e^*} \right)^{1/2} s_y \quad q_y = \left( \frac{m_{et}}{m_e^*} \right)^{1/2} t_y \quad (A-1b)$$

$$k_z = \left( \frac{m_{et}}{m_e^*} \right)^{1/2} s_z \quad q_z = \left( \frac{m_{et}}{m_e^*} \right)^{1/2} t_z \quad (A-1c)$$

In equation (A-1),  $m_e^*$  is given by  $m_e^* = (m_{el} m_{et}^2)^{1/3}$ .

With the above changes of variables, it is found that

$$E_e(\underline{k}) = \frac{\hbar^2}{2m_e^*} s^2 \equiv E_e(s) \quad (A-2a)$$

and

$$E_e(\underline{k} - \underline{q}) = \frac{\hbar^2}{2m_e^*} |\underline{s} - \underline{t}|^2 \equiv E_e(\underline{s} - \underline{t}) \quad (A-2b)$$

Of course, the  $E_e$ 's on the two sides of equation (A-2) represent different functions, but the arguments will always be explicitly stated, and no confusion should result. It is found that  $d^3s = d^3k$  so that  $g_e(q)$  becomes

$$g_e(\underline{t}) = \frac{1}{8\pi^3} \int d^3s \frac{f[(E_e(s) - \mu_e)/k_b T]}{E_e(s) - E_e(\underline{s} - \underline{t})} - \frac{1}{8\pi^3} \int d^3s \frac{f[(E_e(\underline{s} - \underline{t}) - \mu_e)/k_b T]}{E_e(s) - E_e(\underline{s} - \underline{t})} \quad (\text{A-3})$$

Both of the integrals in equation (A-3) can be done in polar coordinates. For both integrals, the  $s_z$ -axis is chosen to lie along the vector  $\underline{t}$ . Thus, for the first integral, one has

$$E_e(\underline{s} - \underline{t}) = \frac{\hbar^2}{2m_e^*} (s^2 + t^2 - 2st\cos\theta) \quad (\text{A-4})$$

For the second integral, one makes the substitution  $\underline{s}' = \underline{s} - \underline{t}$ , whereby  $\underline{t}$  is eliminated from the numerator. Since  $d^3s' = d^3s$ , the primes may be dropped and one then obtains

$$E_e(\underline{s} + \underline{t}) = \frac{\hbar^2}{2m_e^*} (s^2 + t^2 + 2st\cos\theta) \quad (\text{A-5})$$

in the denominator of the second integral.

After performing the angular integrations in equation (A-3), it is found that

$$g_e(\underline{t}) = \frac{1}{4\pi^2} \frac{2m_e^*}{\hbar^2 t} \int_0^\infty s f \left[ \left( \frac{\hbar^2 s^2}{2m_e^*} - \mu_e \right) / k_b T \right] \ln \left| \frac{1 - \frac{2s}{t}}{1 + \frac{2s}{t}} \right| ds \quad (A-6)$$

Equation (A-6) is in a form which begins to resemble the result obtained by Meyer (Meyer, unpublished). The final expression for the dielectric function will be the same as Meyer's, except that scaled arguments will be used.

The reduced Fermi energy,  $\eta_e = \mu_e / k_b T$ , is introduced here. One defines

$$\left( \frac{1}{x_{eo}} \right)^{\frac{1}{2}} \equiv \frac{1}{\hbar t} (2m_e^* k_b T)^{\frac{1}{2}} \quad (A-7)$$

and makes the change of variables  $x = (\hbar^2 / 2m_e^* k_b T) s^2$ . Then equation (A-6) becomes

$$g_e(\underline{t}) = - \frac{1}{8\pi^2} \left( \frac{2m_e^*}{\hbar^2} \right) \frac{t}{x_{eo}} \int_0^\infty f(x - \eta_e) \ln \left| \frac{1 + \frac{1}{2} \left( \frac{x_{eo}}{x} \right)^{\frac{1}{2}}}{1 - \frac{1}{2} \left( \frac{x_{eo}}{x} \right)^{\frac{1}{2}}} \right| dx \quad (A-8)$$

Now, equation (A-8) does not contain the electron-hole pair density,  $n$ . To introduce the density, it is necessary to evaluate

$$n = \frac{v_e}{8\pi^3} \int d^3k f[(E_e(\underline{k}) - \mu_e) / k_b T] \quad (A-9)$$

When the integration in equation (A-9) is performed, and the result is substituted into equation (A-8), equations (20) through (23) for the dielectric function are obtained.

## VITA

Barry Scott Davies was born on 6 September 1951 in New Haven Connecticut. He graduated from high school in Daubury Connecticut in 1970 and attended the Paier School of Art in Hamden Ct, where he studied technical illustration, for one year. He then attended Colby College in Waterville Maine from which he received his Bachelor of Arts degree in physics in 1975. After two years as laborer, he taught physics at Worester Academy in Worcester Massachusetts for one year, and then attended graduate school at the University of Massachusetts (Amherst) until January of 1981. He entered the Air Force Officer Training School in February of 1981 and was assigned to AFIT upon graduation.



REPORT DOCUMENTATION PAGE		READ INSTRUCTIONS BEFORE COMPLETING FORM
1. REPORT NUMBER AFIT/GEP/PH/82D-7	2. GOVT ACCESSION NO. A124 687	3. RECIPIENT'S CATALOG NUMBER
4. TITLE (and Subtitle) EFFECTS OF CONDUCTION BAND ANISOTROPY ON THE EXCITON-PLASMA MOTT TRANSITION IN INDIRECT GAP SEMICONDUCTORS		5. TYPE OF REPORT & PERIOD COVERED MS Thesis
7. AUTHOR(s) Barry S. Davies 2LT		6. PERFORMING ORG. REPORT NUMBER
9. PERFORMING ORGANIZATION NAME AND ADDRESS Air Force Institute of Technology (AFIT-EN) Wright-Patterson AFB, Ohio 45433		8. CONTRACT OR GRANT NUMBER(s)
11. CONTROLLING OFFICE NAME AND ADDRESS AFWAL/AADR WPAFB OH 45433		10. PROGRAM ELEMENT, PROJECT, TASK AREA & WORK UNIT NUMBERS 61102F 2306 R1 01
14. MONITORING AGENCY NAME & ADDRESS (if different from Controlling Office)		12. REPORT DATE December 1982
		13. NUMBER OF PAGES 55
		15. SECURITY CLASS. (of this report) UNCLASSIFIED
		15a. DECLASSIFICATION/DOWNGRADING SCHEDULE
16. DISTRIBUTION STATEMENT (of this Report)  Approved for public release; distribution unlimited		
17. DISTRIBUTION STATEMENT (of the abstract entered in Block 20, if different from Report)  Approved for public release; distribution unlimited		
18. SUPPLEMENTARY NOTES  Approved for public release: IAW AFR 190-17. LYNN E. WOLAVER Dean for Research and Professional Development Air Force Institute of Technology (AIC) Wright-Patterson AFB OH 45433 19 JAN 1983		
19. KEY WORDS (Continue on reverse side if necessary and identify by block number)  Mott Transition, Exciton Ionization, Random Phase Approximation		
20. ABSTRACT (Continue on reverse side if necessary and identify by block number)  A theory is developed for the incorporation of conduction band anisotropy into the analysis of the exciton-plasma Mott transition in indirect gap semiconductors. Ellipsoidal energy surfaces are assumed for the electrons while spherical energy surfaces are retained for holes. Static electron-hole screening in the random phase approximation is assumed.		

The Mott transition is associated with the electron-hole pair density at which the exciton binding energy in the assumed potential is zero. The binding energy is computed variationally.

It is found that the electron anisotropy causes the Mott transition to shift to higher densities. It is also found that, in the absence of screening, the exciton binding energy is not significantly affected by the electron anisotropy. It is thus concluded that the shift to higher densities is due largely to the reduced ability of anisotropic electrons to screen.

END